SEVERE ACCIDENT ANALYSIS OF A SMALL LOCA ACCIDENT USING MAAP-CANDU TO SUPPORT LEVEL 2 PSA FOR THE POINT LEPREAU STATION REFURBISHMENT PROJECT

S.M. Petoukhov, M.J. Brown and P.M. Mathew
Atomic Energy of Canada Limited, Chalk River Laboratories, Ontario, Canada

Abstract

A Level 2 Probabilistic Safety Assessment was performed for the Point Lepreau Generating Station. The MAAP4-CANDU code was used to calculate the progression of postulated severe core damage accidents and fission product releases. Five representative severe core damage accidents were selected: Station Blackout, Small Loss-of-Coolant Accident, Stagnation Feeder Break, Steam Generator Tube Rupture, and Shutdown State Accident. Analysis results for only the reference Small LOCA Accident scenario (which is a very low probability event) are discussed in this paper.

1. Introduction

A Level 2 Probabilistic Safety Assessment (PSA) was performed by Atomic Energy of Canada Limited (AECL) for the Point Lepreau Generating Station (PLGS, a CANDU® 6 reactor) by the Point Lepreau Refurbishment (PLR) Project [1]. An overview of PLGS operations and refurbishment activities was given in [2]. A Level 2 PSA quantified challenges to containment integrity, and the location and species of fission product (FP) releases to the environment. Five representative severe core damage accidents were selected for the Level 2 PSA performed for the PLR Project:

1. Station blackout (SBO);
2. Small loss-of-coolant accident (SLOCA);
3. Stagnation feeder break (SFB) LOCA [3];
4. Steam generator (i.e., boiler) tube rupture (SGTR); and
5. Shutdown state accident (SSA) [4].

Each of the above initiating accidents was analyzed with a reference case and several sub-cases with different availabilities of accident mitigation systems e.g., emergency core cooling (ECC), crash cool-down, steam generator (SG) feedwater. Only results for the reference SLOCA scenario, (Case A), which is a very low probability event, are discussed in this paper.

The MAAP4-CANDU (Modular Accident Analysis Program for CANDU) code v4.0.5A+ [5] was used to estimate:

- The timing of the accident progression and accompanying thermo-physical and thermo-chemical phenomena,
- The effect of safety and normal operational system availabilities,
- Combustible gas sources, hydrogen and carbon monoxide concentrations in containment, and whether burning occurs (depends upon oxygen and steam concentrations),
- FP transport and retention within reactor systems and containment,
- The timing and duration of challenges to containment integrity,

® "CANDU" is a registered trademark of Atomic Energy of Canada Limited.

- The magnitude and nature of FP releases from containment to the environment, and
- The effect of operator actions in mitigating severe accident consequences (reducing challenges to containment integrity and reducing FP releases from the reactor building).

SLOCA reference Case A assumed no operator interventions and credited only a limited number of safety-related systems; other systems were assumed unavailable. A series of sensitivity cases assumed certain system availabilities, to assess their effects on the accident sequence. A total of fourteen cases were analyzed, but the analysis results of only reference Case A are discussed in this paper.

2. Brief Description of the MAAP4-CANDU Code

The MAAP4-CANDU [5] code can simulate severe accidents in CANDU stations, including many of the accident management actions. The code was based on the MAAP4 code developed by Fauske and Associates Inc. (FAI). MAAP4, owned by the Electric Power Research Institute, is used for severe accident analysis of light water reactors. Ontario Power Generation Inc. (OPG) is the MAAP-CANDU code licensee, and AECL holds a sub-license from OPG.

3. Nodalization of the Point Lepreau Generating Station

MAAP4-CANDU simulates the most significant systems and components necessary to demonstrate the overall response of the plant to a severe accident. MAAP4-CANDU tracks the mass and energy content of various heat sinks (liquid, solid and gas) within the reactor building, and the location of FPs - within the fuel, the PHTS and containment, or released to the environment. Fluid momentum within the PHTS is not modelled, but some parameters (e.g., global loop void fraction when phase separation occurs) can be adjusted so the PHTS response better emulates that of dedicated thermalhydraulic codes. However, a primary purpose of MAAP4-CANDU is the availability and use of heat sinks to absorb decay and chemical heat over an entire reactor building, for extended periods well beyond the life of the PHTS.

Some details of the nodalization scheme used to simulate the significant systems and components of PLGS, are described in this section. A more detailed description of the CANDU 6 station nodalization is reported in Reference [1].

The PLGS containment building was represented by 13 volumetric nodes, connected by 31 flow junctions. Concrete containment walls, floors and ceilings, and structural steel, were represented by 94 heat sinks. Adjacent rooms with large connecting openings were lumped together, as were similar heat sinks located in a room or node.

The Primary Heat Transport System (PHTS) was modelled as two loops. Fourteen nodes in each PHTS loop represented the pump discharge lines; reactor inlet headers (RIH); reactor outlet headers (ROH); the inlet piping of two SGs; the hot leg tubes of two SGs; the cold leg tubes of two SGs; and the pump suction lines connected to the cold legs of each SG.

The PLGS reactor core has 380 fuel channels, modelled with 36 characteristic fuel channels (2 loops × 6 vertical core nodes × 3 characteristic channels per vertical core node per loop). The 12 fuel bundles in each characteristic channel were modelled as 12 axial channel nodes, and the calandria tube (CT), pressure tube (PT) and fuel bundle as nine concentric rings.

4. Failure Criteria

A brief description of the failure criteria used is given in the following sections (see [1] and [5] for more details of channel failure criteria). The simulation assumptions are based on best estimates and engineering judgment, and do not reflect the only possible severe accident progression. The sensitivity studies of key assumptions are out of scope of this paper due to space limitations).

4.1 Containment failure criteria

In this study, MAAP4-CANDU used a simple failure junction to model each of two airlocks (equipment and personnel) linking two different nodes in containment (the reactor building) with the environment (service building) [1]. The "environment" represents anything outside the containment boundary.

If the pressure difference exceeded 234.4 kPa (d), between a containment node containing an airlock and the environment, a flow path formed. The opening areas (0.0146 m^2 and 0.0039 m^2) represented the openings anticipated for airlock seal blowouts. The areas and pressure difference were based on small-scale experiments of airlock seals. Both the inner and outer airlock door seals were assumed to fail simultaneously, with no time delay due to the airlock volume between the doors. Other containment failure modes (e.g., containment cracking) were not modelled because the pressures required (>400 kPa) significantly exceeded those of the airlock seal failure.

4.2 Calandria vessel failure criteria

Several criteria are used in MAAP4-CANDU to determine when the calandria vessel (CV) fails. MAAP4-CANDU checks the predicted CV conditions at every time step, to identify if any of the CV failure criteria is met. During each simulation performed for this study, the CV was predicted to fail based on a user input criterion. This criterion assumed CV failure occurred when the calandria vault water level decreased to the level of the top of the terminal debris bed located within the CV, because of insufficient external cooling in that region of the cylindrical CV shell. The CV was conservatively assumed to fail at the bottom, rapidly pouring all the terminal debris into the calandria vault (no debris was assumed to remain within the CV). Additional user-defined CV failure criteria (e.g., uncovery of the top of the vessel, pressurization due to PHTS rupture) could be coded in the input file, but were not considered in this study.

Due to the large surface area of the CV beneath the core debris, and the resulting relatively low heat flux, a water-filled calandria vault was assumed to be adequate for removing the corium heat. The presence of an insulating oxidic crust, a gap between the crust and the CV, and adjacent heat sinks (steel ball-filled end shields and the CV located above the core debris) reduced the heat transferred to the calandria vault water.

4.3 Fuel channel failure criteria

Fuel channel failure is defined as a perforation of its pressure boundaries followed by mass transfer between the inside of the PT and the CV (i.e., both the PT and CT fail). The following fuel channel failure criteria are implemented in MAAP4-CANDU, depending on the PHTS pressure.

At high PHTS pressures, the channel is assumed to fail when a PT and CT creep (i.e., uniform ballooning) criterion is satisfied. When this happens, no fuel channel debris is formed, but the

PHTS depressurizes into the CV. A user could force a channel to fail earlier (e.g., to emulate local hot spots or steep PT thermal gradients), to determine the effect upon the overall severe accident progression, but only the built-in channel failure model was used in the current simulations.

At low PHTS pressures, the fuel channels may fail and form debris, due to local melt-through (Section 4.4). Channel sagging may perforate the CT, allowing CV steam to penetrate into the fuel channel annulus and increasing the channel heat up rate due to the exothermic Zr-steam reaction.

4.4 Fuel channel disassembly criteria

Disassembly is the separation of fuel and channel materials from the original channels. An axial fuel channel node disassembles when the average PT and CT temperature reaches the melting temperature of oxygenated Zr. A disassembled channel node becomes suspended debris, supported by underlying intact channels. These underlying channels are immersed in the remaining moderator, and are cool and strong enough to support the suspended debris until a core collapse criterion is met (Section 4.5). The suspended core debris is tracked by separate components until it moves to the CV terminal debris bed.

4.5 Core collapse criterion

In MAAP4-CANDU, the suspended core debris rapidly relocates (collapses) to the bottom of the CV when the total suspended debris mass exceeds a user-specified value. A mass of 25,000 kg of suspended debris, per PHTS loop, was used in the current analysis, based on an assumption of the pull-out strength of cooled calandria tubes.

4.6 Fission product release criteria

MAAP4-CANDU models the fuel elements as a mixture of UO_2 and the fuel sheath material. The fuel sheath is modelled to fail if the combined fuel sheath/UO_2 temperature of a radial channel node (i.e., fuel ring) reaches a user-defined value (1000 K in this analysis, based on PHEBUS and BTF test results).

Fission products from the fuel matrix are modelled to be released based on fractional release models driven by the fuel temperature. The initial FP distribution is based upon the local heat generation at normal operating conditions. MAAP4-CANDU has no model of radioactive decay, but uses a total core decay heat curve. The decay heat is distributed amongst the FP groups based on a single time (the decay heat distribution does not change significantly past ~6 hours since reactor trip). MAAP4-CANDU v4.0.5A+ assumes that no FPs are released from the terminal debris bed that accumulates on the bottom of the CV, because of the barrier provided by the top debris crust. Also, the CV is dry by the time the terminal bed heats up enough to release FPs, so there is no steam flow through the debris to transport the FPs.

5. Key Input Parameters for the Point Lepreau Generating Station

The key PLGS input parameters used in this study are presented in Table 1 of Reference [1]. In these analyses, the inventories of only the radioactive FPs were input to MAAP4-CANDU.

6. Accident Description and Analysis Assumptions

6.1 Brief description of the Small Loss Of Coolant Accident

The following describes the basic severe accident sequence anticipated for the small LOCA scenarios in this report, and some of the effects of different assumptions. The processes or phenomena described in this section are modelled by MAAP4-CANDU, some in greater detail or sophistication than others. Several complex processes of the severe core damage portion of the accident (core debris formation and movement, debris-CV walls interaction, etc.) are based on engineering judgement due to a lack of experimental data. Some of the MAAP4-CANDU modelling assumptions are briefly described as they have a significant effect upon the accident progression or consequences; Section 6.2 contains more details of MAAP4-CANDU assumptions.

The anticipated accident sequence starts with a small loss of coolant, and progresses to core damage and disassembly (i.e., a severe accident) because of the loss of: i) long-term ECC, ii) moderator cooling, and iii) shield and calandria vault cooling. Some simulations performed for this (PLR) project credited safety-related system functions (e.g., SG feedwater, high and medium-pressure ECC injection, crash cool-down), but these tended only to delay the event timing and will not be discussed further in this section.

The basic accident sequence is as follows:

a) Beginning: reactor is at full power and pressure.

b) Initiating event: rupture of one RIH in PHTS Loop 1. Break equivalent to twice the cross-sectional area of a large inlet feeder (i.e., guillotine break of the large feeder) and is located at underside of RIH.

c) Containment pressure rises, due to hot primary coolant from break, and trips reactor within ~9 s of initiating event.

d) PHTS pressure in broken Loop 1 decreases; coolant from pressurizer and intact Loop 2 flows into Loop 1 via common piping.

e) PHTS loops and pressurizer are isolated from each other, ending flow of coolant from intact Loop 2 to broken Loop 1. Loop 1 coolant continues to vent from break.

f) SGs provide heat sinks for both loops, provided enough primary coolant is available to transport heat from fuel to SGs. Loop 1 SG heat sink capability rapidly decreases as coolant level drops. Remaining Loop 1 coolant boils off by fuel decay heat, and the steam vents out of RIH break.

g) Loop 1 channels are now dry, so fuel heats up. Channels are surrounded by cool moderator that limits channel and fuel heat up. Fuel sheaths may be hot enough to oxidize with Loop 1 steam, producing hydrogen (some vents into containment via RIH break).

h) Loop 2 continues to be well cooled by its SGs, because sufficient primary coolant remains after loop isolation occurs. Loop 2 cooling ceases after SG secondary side water inventories boil off. If auxiliary feedwater is available, it prolongs heat removal from Loop 2 fuel channels; the availability of auxiliary feedwater has limited effect on Loop 1 cooling, because Loop 1 primary coolant is lost via RIH break.

i) After loss of Loop 2 SGs, Loop 2 coolant heats up and pressurizes until liquid relief valves (LRVs) open at 10 MPa. LRVs vent primary coolant into the degasser condenser (DC); when DC pressure exceeds ~10 MPa, it vents to containment. DC was not modelled in present simulations, so LRVs were modelled to vent directly to containment.

j) Loop 2 coolant boils off and vents out LRVs, so Loop 2 water level decreases and fuel channels begin to dry out. Loop 2 pressure remains high, because loop is still intact, so dry channels overheat and strain outwards (balloon) until at least one fails.

k) Loop 2 fuel channel failure depressurizes loop. Flow of Loop 2 coolant heats and pressurizes CV, and CV rupture disks open. Hot Loop 2 steam and boiling moderator expel some moderator out CV relief ducts and into containment.

l) All fuel channels in both loops dry out, and remaining moderator is main heat sink for channels. As moderator level decreases (expulsion and boil off), upper fuel channels become suspended in steam, which is inadequate to cool them. Note that PHTS Loop 1 voided well ahead of Loop 2 but both loops currently have similar conditions – hot and dry (unless auxiliary feedwater available to cool Loop 2 for longer).

m) Fuel and fuel channels heat up further, and sections begin to disassemble from channels. Debris is likely coarse. Bundle-length sections of fuel and fuel channel are too large to slip between lower intact channels, so solid debris remains supported by lower channels. Lower channels remain strong (they are immersed in remaining moderator).

n) Suspended debris is un-cooled, and heats up from decay heat and Zr-steam oxidation. Some debris melts and trickles down into remaining moderator, solidifying on CV bottom. Some solid debris may relocate downwards, stopped by lower fuel channels or reaching CV bottom.

o) Moderator level continues to decrease, due to heat from still-immersed fuel channels and from debris at CV bottom. More channels are uncovered, heat up, form debris and no longer can support overlying debris. Thus suspended debris cascades down, stopped by lower, still-strong channels.

p) Suspended debris load exceeds the support capability of underlying channels, and supporting channels plus suspended debris collapse to CV bottom. Remaining moderator quenches debris, generating large quantity of steam that vents to containment.

q) Steam generated by core collapse pressurizes containment; pressure rise rate depends upon collapse speed, mass of collapsed channels and debris, and mass of remaining moderator. Slower collapse allows more condensation on containment structures, decreasing peak pressure. In M4C, core collapse is rapid single event, although each PHTS loop treated separately (i.e., one, both or no loops may collapse, depending upon simulation progression).

r) Much of fuel and fuel channels now on CV floor, moderator has boiled off. Calandria vault water is the only remaining large heat sink. End shield water provides small heat sink, but its initial mass is only 2.6% of calandria vault water, and is closely coupled (thermally) to fuel channels. Thus, end shield water boils off quickly and probably completely depleted by core collapse. End shield heat up and pressurization opens rupture disks shared with calandria vault.

s) Calandria vault water surrounds CV, providing large heat sink for debris on CV bottom. Some CV debris heats up and melts, and some forms solid crust on top, sides and bottom. The calandria vault water boils off and water level declines.

t) When calandria vault water level decreases to same elevation as top of CV debris, CV heats up locally. The CV would melt-through first in some location, depending upon local heat transfer from non-uniform debris bed, and upon local thickness of solid debris crust in CV.

u) Molten debris relocates out of CV hole into calandria vault, where it quenches in remaining calandria vault water. In the MAAP4-CANDU simulations, CV assumed to fail when calandria vault water decreases to elevation of top of debris in CV, and debris rapidly relocates into calandria vault. This assumption is conservative, since relocation process will take some time. Likely, that failure location will grow in size, and thus relocation process and mass flow into calandria vault will be slower than assumed here. Experimental data lacking to develop appropriate model for this process. Similar to core collapse, rate and amount of debris movement (and thus energy content) changes rate of steam generation and thus containment pressurization.

v) Debris in calandria vault boils off remaining calandria vault water; debris heats up and begins interacting with concrete floor of calandria vault (molten core – concrete interaction or MCCI). Calandria Vault floor eroded until it fails.

w) Molten core and concrete relocates into water-filled basement. Relocation rate is factor in steam generation rate and containment pressurization. Like CV failure, debris relocation assumed rapid and probably conservative. Containment walls already hot from previous steam condensation, so condensation less effective at reducing containment pressure during calandria vault failure than during previous steam generation periods (e.g., CV failure). Given lower condensation capability, steam generation rate has less effect on maximum containment pressure during calandria vault failure than during previous major quench events (i.e., core collapse and CV failure).

The airlock seals (containment) may fail during many of the events listed above, in particular during periods of rapid steam generation (*q*: core collapse, *u*: CV failure, *w*: calandria vault failure) that produce pressure peaks.

During many of the accident stages, core debris can release FPs to the containment. The release rate can be significant during the initial fuel heat up (via sheath failures), the suspension of hot core debris in the CV, and the core-concrete interaction.

The above severe accident events and processes, illustrate many occasions where user-input and code assumptions have a major influence upon the accident sequence and timing. For example, an earlier core collapse reduces the time that debris remains suspended in the CV, thus reducing the amounts of hydrogen produced and FPs released in that stage of the accident. It would also reduce the pressure peak caused by the collapsed core being quenched, perhaps avoiding containment failure at that time.

6.2 Analysis assumptions

The severe accident (SLOCA) initiating event was the failure of one RIH in PHTS Loop 1, with a total break area of 0.00537 m^2. This break, equivalent to about 2.5% of twice the cross-sectional area of the reactor inlet header, corresponds to a guillotine break of a large inlet feeder (i.e., twice the cross-sectional area of a large feeder). The break elevation was set at the bottom of the RIH, 10.325 m above the inside bottom of the CV. The simulations were run up to 500,000 s (138.9 h).

All the SLOCA-initiated severe accidents were simulated with the following assumptions:

a) Total heat generation in reactor, at time 0, assumed to be 2155.9 MW (th). This heat includes heat deposited in moderator by gamma heating; MAAP4-CANDU requires this total as an input, not just heat transferred from fuel to PHTS coolant.

b) Class IV and class III electrical power available.

c) Reactor shutdown credited (reactor trips on high containment pressure of 3.45 kPa (g)).

d) Moderator, shield and shutdown cooling systems not credited.

e) Main SG feed water unavailable after reactor tripped.

f) There are no main steam isolation valves (MSIVs) in PLGS. No MAAP4-CANDU models, of CANDU secondary side downstream of the SGs, were used for this analysis. Therefore, it was necessary to close off non-existent secondary side at 0 s by using MSIV model. Since reactor did not trip for 9 s from simulation start, this pressurized secondary side of SGs, which vented some steam through main steam safety valves (MSSVs). This had an insignificant effect on results.

g) Containment leakage modelled by an opening to environment that allowed 2.5% containment volume to leak out per 24 hours, given a pressure difference of 124 kPa.

h) Low-pressure ECC injection not credited.

i) PHTS loop isolation system credited. Isolation assumed complete 30 s after loop isolation signal was generated by PHTS loop pressure decreasing to 5.52 MPa (g). The 30 s delay represented the valve closing time from initiation to complete loop isolation, but MAAP4-CANDU only models loop isolation as on or off.

j) AECL passive autocatalytic recombiners (PAR) credited. Total of 19 PARs: 8 in containment Node 1 (basement), 1 in Node 2 (stairwell to SG room), 1 in Node 5 (portions of floors 1, 2, 3 and 4), 8 in Node 8 (lower SG room), and 1 in Node 9 (moderator service area).

k) The LRVs and pressurizer relief valves modelled to discharge PHTS coolant directly to containment. In reality, these valves discharge into DC; but DC was not modelled in these analyses. Lack of DC model is conservative, because it would have provided additional 20 m^3 volume to contain high pressure PHTS steam or liquid from intact loop, delaying and reducing coolant venting (from intact loop) into containment. This would have slowed containment pressurization due to primary coolant from intact loop, but not from broken loop. Some FPs could be deposited in DC, but only from intact Loop 2.

l) Moderator cover gas system bleed valves, connecting CV and vapour recovery system, operable for first 7,200 s, then failed open after 7,200 s because (assumed their air reservoirs depleted). These valves allowed some moderator (water or steam) to leave CV.

m) The SG main steam safety valves were available; they opened and closed at their set point (5.11 MPa) to relieve the SG secondary side pressure.

n) No operator interventions were credited explicitly, except for crediting additional SG auxiliary feedwater in Cases C and E, which would require operator actions.

o) PHTS coolant initially modelled as single-phase liquid (i.e., the user-input initial void fraction `VFPS0` = 0). As void fraction increased, due to break or boil off, coolant was modelled as homogeneous two-phase fluid. When PHTS loop void fraction increased to user-input `VFSEP`, PHTS coolant in that loop separated into two phases – water below and steam above – and water was tracked in separate PHTS pools (corresponding to PHTS nodes and fuel channels). If PHTS loop refilled by ECC injection, water pools would rejoin; when PHTS loop void fraction decreased to `VFCIRC` (user-input), coolant again modelled as single-phase fluid. For these simulations, `VFSEP` = 0.5 and `VFCIRC` = 0.2.

p) Containment isolation assumed to be effective from beginning of accident. In reality, this system would operate if containment pressure increased to 3.5 kPa (g); in SLOCA simulations this happened within ~6 s after break began.

In addition to the above assumptions, which applied to all the SLOCA simulation cases, six system capabilities were varied according to the individual cases:

a) SG crash cool-down: available or unavailable (unavailable in reference case).
b) High and medium pressure ECC injection: available or unavailable (unavailable in reference case).
c) Auxiliary SG feed water: available or unavailable (unavailable in reference case).
d) Airlock seals: Containment failure assumed to occur by a blow out of airlock seals. In most cases, failure was assumed to occur at 234 kPa (g), but in one case this was assumed to occur at 334 kPa (g). See Section 4.1 for details.
e) Local air coolers (LACs): unavailable or available. Sensitivity cases performed to determine minimum number of LACs necessary to maintain containment (i.e., airlock seal) integrity for >72 h. Performance of LACs may be underestimated in this analysis. It is recommended that a check be performed against GOTHIC prior to using these results in Level 2 PSA work (unavailable in reference case).
f) Containment dousing: available, but total capacity and maximum flow rate were different in some cases.

7. Major Analysis Results

7.1 Case A – Primary heat transport system and steam generator response

In the reference simulation (Case A), the PHTS Loop 1 RIH break began at 0 s, so the loop started to depressurize (Figure 1). The reactor tripped at 9 s (the reactor building high-pressure set-point was reached), rapidly decreasing the input heat. The SGs continued to remove large amounts of heat by boiling the secondary inventory and venting the steam through the MSSVs, thus cooling the PHTS coolant. The net result was that the PHTS pressure dropped rapidly due to the combination of the coolant loss via the break, fission power loss and the SG availability as a heat sink.

The break flow began at ~190 kg/s (Figure 2) decreasing as the PHTS pressure dropped and the PHTS void fraction increased. The Loop 1 PHTS coolant changed from a homogeneous mixture to separate water and steam phases at 340 s, because the overall Loop 1 void attained 50% (`VFSEP` = 0.5). This separation briefly increased the mass flow through the break, until the water level decreased below the break height. When that occurred, the break flow became entirely steam, sharply dropping the mass flow rate, which then decreased more gradually due to the Loop 1 depressurization.

Prior to PHTS loop isolation, the pressures of both loops decreased in step with each other, since the loops were linked together via the pressurizer interconnect until loop isolation occurred at 285 s (the loop isolation signal was generated after the PHTS pressure <5.62 MPa (a)).

The SGs continued to provide large heat sinks for the PHTS, and the secondary side pressures remained close to the MSSV set point pressure of 5.11 MPa (a) for ~12,000 s (Loop 1) and ~7,000 s (Loop 2) (Figure 3). When the amount of core heat transferred to the SGs decreased significantly, the SGs cooled gradually by exposure to the cooler containment, depressurizing during the remaining simulation to 500,000 s (Figure 3).

Following PHTS loop isolation, the water mass in the intact Loop 2 stayed constant at ~36,500 kg because there was no Loop 2 break (Figure 4). The Loop 2 pressure remained approximately constant until ~2,800 s (0.8 h), when the Loop 2 SGs could no longer remove all the decay heat because the secondary side water level was decreasing (Figure 5). By 3,073 s (0.9 h) the secondary side water in the Loop 2 SGs was depleted, so they ceased to be heat sinks for Loop 2; as a consequence, the Loop 2 water boiled and the pressure increased (Figure 1).

When Loop 2 reached 10.16 MPa (a) at 3488 s (1.0 h), the LRVs opened to relieve the pressure, but they were inadequate to vent enough volume of homogeneous two-phase coolant to stop the pressure rise (Figure 1). The Loop 2 PHTS coolant separated into water and steam at 4,166 s (1.2 h). Soon afterwards, the PHTS water level dropped below the LRV elevation, so the LRV flow became entirely gas; this relieved the Loop 2 pressure much more rapidly than water flow through the LRVs. The maximum Loop 2 pressure reached 15.3 MPa (a) before declining to about 10.16 MPa (a) at 5,857 s (1.6 h). From then on, the LRVs opened and closed to relieve the Loop 2 steam pressure, and maintained a constant pressure until a fuel channel ruptured.

In PHTS Loop 2, a continuous loss of inventory through the LRVs and heating from the decay heat resulted in fuel bundles uncovering inside the fuel channels at 4,572 s (~1.3 h). Fuel channels became dry (i.e., less than 1 kg of water remaining in the fuel channel) in Loop 2 at 7,275 s (~2.0 h) (Table 1), and fuel elements heated up. A heat-up of the pressure tube and calandria tube at a PHTS pressure greater than 10 MPa, resulted the rupture of both tubes. This fuel channel rupture caused a rapid coolant blow-down from the PHTS into the CV and Loop 2 pressure drop at 7,355 s (~2 h).

7.2 Case A – Fuel and fuel channel response

The first fuel channel (characteristic channel #4) dried out in Loop 1 at 4,604 s (~1.3 h), while the first Loop 2 fuel channel dried out at 7,275 s (~2 h). Uncovering fuel elements inside the fuel channel was the result of: (1) the loss of PHTS coolant through the openings in the RIH break and in the broken channel (in PHTS Loop 2), and (2) coolant boil-off because of the core decay heat. The temperature of the pressure and calandria tubes, as well as fuel ring #1 for bundle #7 in characteristic channel #1 is presented in Figure 6. This channel was located in the top core node of PHTS Loop 1, and dried out at 4,796 s (~1.3 h).

When the pressure and calandria tubes reach disassembly conditions (Section 4.4), fragments of the fuel channel relocated into “holding bins” and stayed there temporarily in the form of a suspended debris bed. The core material in the suspended debris bed heated up further due to core decay heat and the Zr-steam reaction.

When the suspended debris bed mass in the core exceeds a user-specified value (25,000 kg per PHTS loop is used in the present work, Section 4.5), the core material in the suspended bed and most of the intact channels of the damaged Loop 1 relocated to the CV bottom. This process of massive relocation of core material to the CV bottom happened at ~18,600 s (~5.2 h) for Loops 1 and 2. The dynamics of channel disassembly and relocation phenomena are represented in Figure 7. The mass of UO_2 in the intact core-material decreased rapidly at ~18,600 s (~5.2 h) for Loops 1 and 2. It is the result of material transfer to the holding bins and relocation of molten material to the CV bottom.

7.3 Case A – Calandria vessel response

The moderator level (Figure 8) rose slowly from 8.05 m (measured from the CV bottom) at the beginning of the accident. The rise occurred because the moderator cooling system, which was assumed inoperable for this case, no longer removed the heat from the channels so the moderator swelled from thermal expansion. At 6,508 s (1.8 h), the moderator cover gas system bleed valves opened, at a pressure differential of 29 kPa between the CV and the containment, and stayed open. This slowed the rise in the CV pressure (Figure 9) and in the two-phase moderator level by venting gas and steam (Figure 10).

When the Loop 2 fuel channel ruptured at 7,355 s (2.0 h), the steam blown into the moderator increased the two-phase level (Figure 8) and also pressurized the CV. The moderator reached saturation conditions at 7,508 s (2.1 h); however, it took until 9,210 s (2.6 h) for the CV rupture disk to open to containment, because the containment pressure was also increasing from the continued loss of steam out the RIH break. After the CV rupture disk opened, the CV pressure was a little higher than the containment pressure, due to the steam flow out the relief duct.

Following the CV rupture disk opening, the moderator boiled extensively because it was already saturated and the pressure had decreased to approximately containment pressure. The net result was an expulsion of ~35% of the moderator (by mass) into containment. When the expulsion was over at ~9,800 s (~2.7 h), the two-phase moderator level was 6.8 m above the CV bottom. This was still above the topmost characteristic fuel channel, but heat from the fuel channels continued to boil the moderator and so the level dropped. By 24,976 s (6.9 h), the CV was dry on the inside but cooled on the outside by the water in the surrounding calandria vault.

Figure 11 shows the total corium mass (particulates, corium crust, plus molten corium), the mass of the corium crusts (bottom, side and top surfaces) and the mass of particulates in the CV. Particulates were solid core debris formed during fragmentation of the molten core material (pouring down from the suspended debris) in the remaining moderator. A crust, in the range 5 to 10 cm thick, formed on the CV walls as the core material finished relocating to the CV bottom. After the CV water was depleted, the core debris in the CV started to heat up; eventually the particulates melted to form the molten debris pool at ~40,000 s (~10.1 h, Figure 11).

The calandria vault water level decreased to the elevation of the top of the CV debris bed at 139,070 s (38.6 h), so the CV wall failed at the bottom of the vessel (Section 4.2). All the core debris then relocated out of the CV and onto the calandria vault floor; it was assumed that no crust remained in the CV. An energetic interaction of corium and calandria vault water was predicted, when the CV cylindrical shell failed.

7.4 Case A – Calandria vault and end shields response

The pressure (Figure 9) and water level (Figure 10) in the calandria vault and end-shields increased gradually after the initiating event, due to the unavailability of the shield and moderator cooling systems and the resulting thermal expansion of the calandria vault water. The calandria vault and end-shields are connected via combined vent lines, which can relieve over-pressure via rupture disks. At 10,282 s (2.9 h), these rupture disks burst (Table 1). Steam was discharged from the end shields to the containment, resulting in a decrease of the calandria vault and end-shield water levels. The water in the calandria vault began to boil off at about 38,891 s (10.8 h), which resulted in a gradual water level decrease.

As described in Section 7.3, the CV failed at 139,070 s (38.6 h). As a result, all the core debris poured out onto the calandria vault floor (Figure 11). The calandria vault water continued to boil off, at a faster rate than previously due to the water contacting a larger surface area of core debris, and at 155,553 s (43.2 h) the last of the calandria vault water boiled off (Table 1).

After the loss of the calandria vault water heat sink the corium temperature increased due to the decay heat, and corium - concrete interaction began at 164,218 s (45.6 h). When the eroded depth of the concrete floor reached 2 m at 403,152 s (112 h), the calandria vault was considered failed. At that time, the debris from the reactor vault relocated to the reactor building basement, there it was quenched in the water pool. This resulted in a final containment pressure spike (Figure 9).

7.5 Case A – Containment response

Figure 9 shows the pressure in the lower half of the SG enclosure, which is one of the biggest containment compartments. Initially, the containment pressure was about 101 kPa (a). The rapid increase of the containment pressure, during the initial period of the accident, was due to the hot PHTS coolant discharging through the PHTS Loop 1 RIH break and flashing to steam. Further events added to the containment pressurization: at 3,488 s (1.0 h) PHTS Loop 2 coolant began to be discharged through the PHTS LRVs into the containment; a CV rupture disk opened at 9,210 s (2.6 h); and the calandria vault rupture disk opened at 10,282 s (2.9 h). The moderator had begun to boil at 7,508 s (2.1 h) and a Loop 2 fuel channel ruptured at 7,355 s (2.0 h), so when the CV rupture disk burst, the Loop 2 PHTS coolant plus steam from the boiling moderator discharged into containment via the open CV relief duct; this caused a sharp increase in containment pressure.

The rapid increase in containment pressure at ~18,600 s (5.2 h) was caused by the core collapsing to the CV bottom at 18,585 s (5.2 h), followed by steam generation as the remaining moderator quenched the debris. This pressurization blew out both airlock seals at 18,839 s (containment failure criterion of 234 kPa (g), Section 4.1). The containment pressure continued to increase for a few hundred seconds after the airlock seals blew out, because the steam generation rate exceeded the sum of the steam/gas mixture discharge rate to the environment and the rate of condensation within containment.

The containment pressure continued to decrease until, at 38,891 s (10.8 h), the calandria vault water reached saturation conditions. The increased steam flow into containment exceeded the sum of the efflux through the blown out airlock seals and the condensation within containment, so the containment pressure began to increase again.

The containment pressure increased slowly (Figure 9) after the calandria vault water began to boil; it reached a maximum of 150.1 kPa (a) at 88,280 s (24.5 h), when the steam generation matched the discharge plus the condensation in containment. The containment pressure then decreased to about atmospheric pressure by ~170,000 s (~47 h), because the calandria vault water was depleted by 155,553 s (43 h) and thus the steam generation ended.

The containment pressure rapidly increased at 403,152 s (112 h), due to corium relocating into the basement after the calandria vault failed, followed by steam generation as the hot core debris was quenched in the basement water. The containment pressure decreased soon after, mainly because of the steam discharge through the airlock seals. Also, the corium was quenched in the basement water (steam generation ceased) and steam condensed on the containment walls and internal structures. The simulations did not employ a criterion for a large-scale failure of containment, only one for the airlock seals blowout.

7.6 Case A – Fission product release and distribution

The initial inventory (radioactive isotopes only) of noble gases (Kr and Xe) in the core was 1.04 kg. After 4,604 s (~1.3 h), when the first fuel channels became dry (i.e., less than 1 kg of water remaining in the fuel channel) and the fuel element temperatures exceeded 1000 K, FPs began to be released from fuel elements (Section 4.6). Most of the noble gases were released into the CV from the fuel and the suspended debris bed during core disassembly (~3.3 h to ~5.2 h). The noble gases escaped to the containment through the burst CV rupture disks. From containment, some noble gases escaped to environment (Figure 12) via containment leakage and through the blown out airlock seals. Eventually all noble gases were released to the environment, following containment failure at 5.2 h.

Figure 13 shows the mass of radioactive CsI released from fuel and debris in-vessel (inside the CV) and from the containment to the environment. The initial inventory of CsI in the core (radioactive isotopes) was 17.1 kg. Fission products were released to the CV from the PHTS and from the suspended debris bed. When the CV rupture disks burst open at ~2.6 h, FPs could now be transported from the CV into containment. It was assumed that the corium crust, formed in the CV, prevented significant FP releases. When the CV failed, the crust failed but the debris was quenched in the remaining calandria vault water, so any further FP releases would have been very low. After the calandria vault water was depleted at 43.2 h, the corium heated up and reacted with the concrete starting at 45.6 h; FPs were released ex-vessel (outside the CV) (Figure 13).

At the end of the simulation (500,000 s), the total mass of Cs, Rb and I released to the environment, in the form of CsI, CsOH and RbOH (radioactive isotopes), was 1.5 kg or 8.6% of the initial inventory of these isotopes.

7.7 Case A – Hydrogen release

Hydrogen was released by steam reacting with Zr in hot and dry fuel channels, and in the suspended debris beds of both PHTS loops. The first fuel channels dried out in Loop 1 at 4,604 s (~1.3 h), and in Loop 2 at 7,275 s (~2.0 h). Steam inside the channels reacted with the Zr fuel cladding and inner surface of the Zr pressure tube. This exothermic reaction produces hydrogen, and the reaction rate increases at higher temperatures. The hydrogen production increased after core disassembly started at ~3.3 h (Loop 1) and at ~3.6 h (Loop 2). At ~6.9 h the CV was dry, so hydrogen production significantly decreased with the lack of fresh steam. A very small amount of hydrogen was produced from the remaining intact channel stubs still located in the CV. The solid crust formation, on top of the CV debris bed, was assumed to prevent steam access to the debris.

The total amount of hydrogen produced during the core heat up and disassembly was 207 kg, which was produced inside of the PHTS loops and from the debris suspended inside the CV. This corresponds to ~11.6% of the initial Zr core inventory being consumed.

No hydrogen or carbon monoxide burning in containment was predicted in Case A, due largely to the airlock seals failure and the subsequent steam generation purging containment.

7.8 Sensitivity cases

As mentioned, a total of fourteen Small LOCA cases (including reference Case A) were analyzed for the PSA Level 2 activities for PLGS Refurbishment Project. Sensitivity cases credited various plant safety-related features/operator actions. The results of the sensitivity cases are beyond the scope of this paper and will be published separately.

8. Summary

A series of fourteen simulations were run to assess the consequences of a severe accident, beginning with a small LOCA, in the Point Lepreau CANDU 6 generating station. This was done for a Level 2 probabilistic safety assessment, for the PLGS refurbishment. The accident began with a guillotine break of a feeder where it was attached to its reactor inlet header, while the reactor was at full power. The simulations were run with the severe accident analysis code MAAP4-CANDU v4.0.5A+, using the PLGS specific parameter file. This paper discusses major results of SLOCA reference Case A, which assumed most safety-related plant systems were not available:

Unavailable: Main and auxiliary SG feedwater, emergency water supply, moderator cooling, shield cooling, shutdown cooling, and emergency core cooling.

Available: Reactor shutdown, dousing spray, class III and class IV power, AECL PARs, SG main steam safety valves.

In reference Case A, severe core damage began at 3.3 hours, the moderator was depleted (boiled off) in the CV at 6.9 h, containment failed at 5.2 h, and the CV failed at 38.6 h. The total release of radioactive isotopes of Cs, Rb and I was 8.6% of their initial inventory. Almost the entire initial noble gas inventory in the core was transported with the containment atmosphere to the environment, primarily after the containment failure. No hydrogen/carbon monoxide burning was predicted in the containment.

9. Acknowledgements

Authors wish to thank the following individuals for their contribution to the paper:

Chan Y. Paik (FAI), Liliana Comanescu (Candu Energy), Mark Yandt and Barbara Pruszkowski (all of AECL); Ghulam Khawaja (OPG), and all reviewers for their helpful discussions and comments.

10. References

[1] S.M. Petoukhov, M.J. Brown and P.M. Mathew, "MAAP4-CANDU Application to the PSA Level 2 for the Point Lepreau Nuclear Generating Station Refurbishment Project", Proceedings of the 30th Annual Canadian Nuclear Society Conference: "New Nuclear Frontiers", Calgary, Alberta, Canada, 2009 May 31-June 3.

[2] R. Eagles, "Point Lepreau Generating Station Refurbishment Project - Update and Status", Proceedings of the 28th Annual Conference of the Canadian Nuclear Society, Saint John, New Brunswick, Canada, 2007 June 3-6.

[3] S.M. Petoukhov and G.M. Khawaja, "Severe Accident Analysis Of Stagnation Feeder Break Scenarios Using MAAP4-CANDU For Application To The Level 2 PSA For The Point Lepreau Station Refurbishment Project", Proceedings of the 32nd Annual Conference of the Canadian Nuclear Society, Niagara Falls, Ontario, Canada, 2011 June 5-8.

[4] S.M. Petoukhov, M.J. Brown and P.M. Mathew, "Severe Accident Analysis Of Shutdown State Accident Using MAAP4-CANDU To Support Level 2 PSA For The Point Lepreau Station Refurbishment Project", Proceedings of the 32nd Annual Conference of the Canadian Nuclear Society, Niagara Falls, Ontario, Canada, 2011 June 5-8.

[5] P.M. Mathew, S.M. Petoukhov and M.J. Brown, "An Overview of MAAP4-CANDU Code", Proceedings of the 28th Annual Conference of the Canadian Nuclear Society, Saint John, New Brunswick, Canada, 2007 June 3-6.

Table 1
Sequence of Significant Events for Small Break LOCA Scenario Reference Case A

Time (hr)	Time (s)	Event
0.0	0	Turbine main stop valves closed
0.0	0	Moderator cooling and circulation off
0.0	0	Shield cooling system off (cooling and circulation)
0.0	9	Reactor trip due to high pressure in lower SG room
0.0	9	SG main feedwater pumps off (auxiliary feed water not available in Case A)
0.0	42	Dousing starts
0.0	74	Pressurizer empty
0.1	285	PHTS loops isolated when PZR isolated (30 s after loop isolation signal)
N/A	N/A	Crash cool-down start (crash cool down unavailable in Case A)
N/A	N/A	Auxiliary feedwater starts (AFW unavailable in Case A)
0.2	701	Dousing exhausted (dousing max flow rate is 2,142 kg/s)
0.9	3,073	SG secondary sides are dry, Loop 2
N/A	N/A	SG secondary sides are dry, Loop 1 (Loop 1 drained before it could boil off the SG inventory)
1.0	3,488	LRVs open for first time, PHTS Loop 2
1.3	4,604	At least one channel is dry Loop 1 (complete boil-off) – Channel 4
1.8	6,508	CV bleed valve open
2.0	7,275	At least one channel is dry Loop 2 (complete boil-off) – Channel 4
2.0	7,355	Pressure and calandria tubes are ruptured Loop 2 – Channel 4
2.1	7,508	Moderator reaches saturation temperature
2.6	9,210	CV rupture disk 1 is open
2.9	10,282	Calandria vault rupture disk open, connecting to SG room
3.3	11,844	Beginning of the core disassembly, Loop 1
3.6	12,795	Beginning of the core disassembly, Loop 2
5.2	18,577	Loop 2 massive core debris relocation (core dump) to CV bottom
5.2	18,585	Loop 1 massive core debris relocation (core dump) to CV bottom
5.2	18,839	Containment failed (both airlock seals blew out)
6.9	24,976	Water is depleted inside CV
10.8	38,891	Water in calandria vault reaches saturation temperature
38.6	139,070	CV bottom failed
38.6	139,076	Energetic core-debris steam interaction occurred in calandria vault
43.2	155,553	Water is depleted inside calandria vault (Node 10)
45.6	164,218	Molten corium-concrete interaction begins in calandria vault
112	403,152	Calandria vault floor failed because of concrete erosion

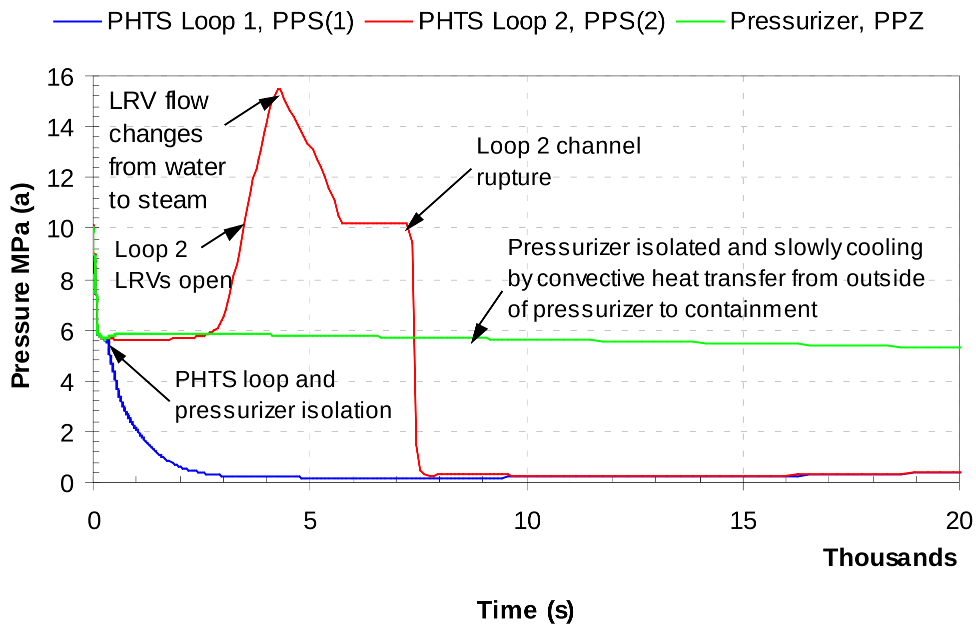

Figure 1 Primary System and Pressurizer Tank Pressure, Case A (0 – 20,000 s)

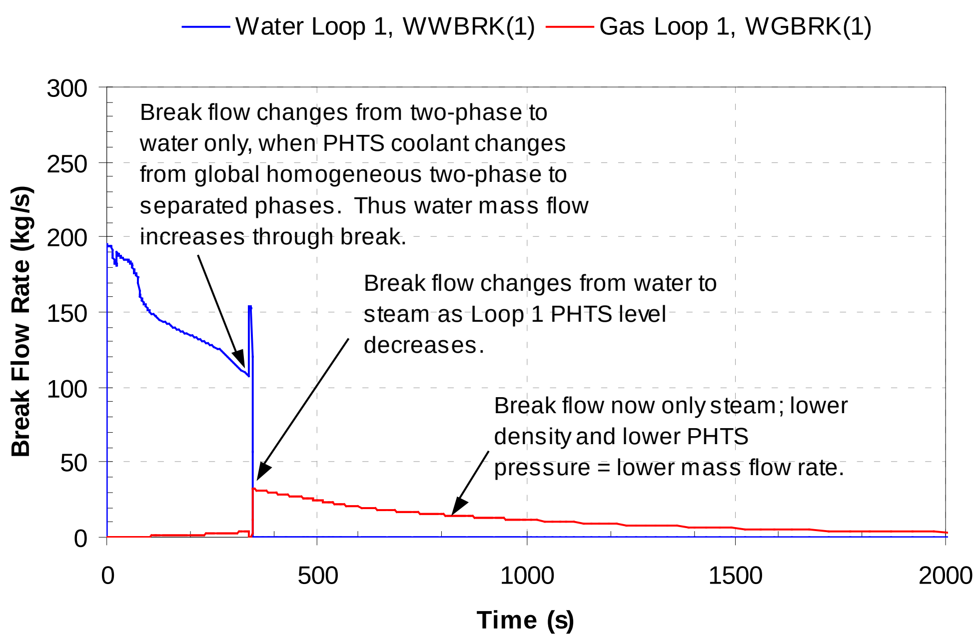

Figure 2 RIH Break Flow Rate, Case A (0 – 2,000 s)

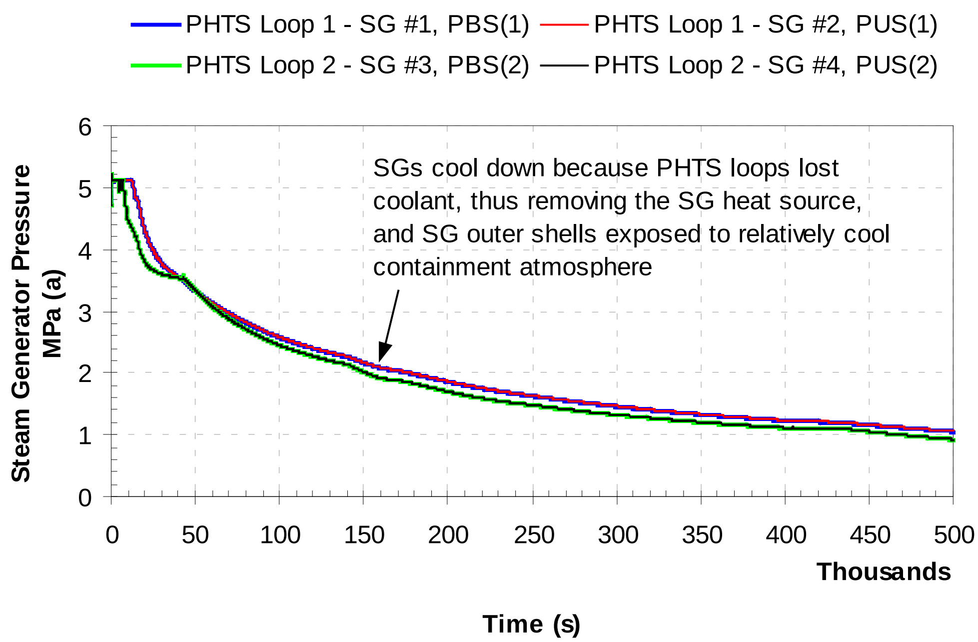

Figure 3 Steam Generator Secondary Side Pressure, Case A (0 – 500,000 s)

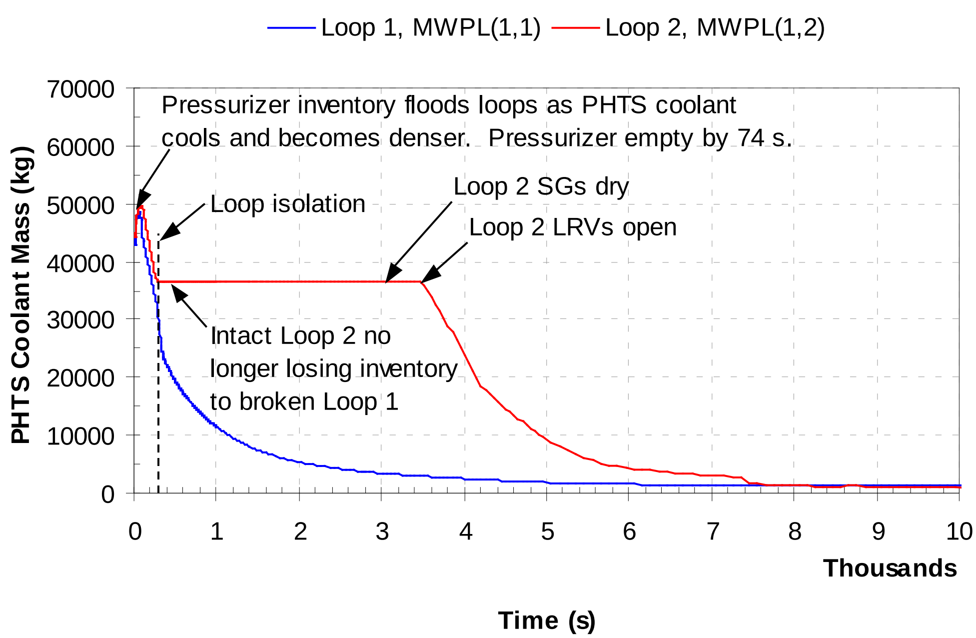

Figure 4 Water Mass in PHTS Loops, Case A (0 – 10,000 s)

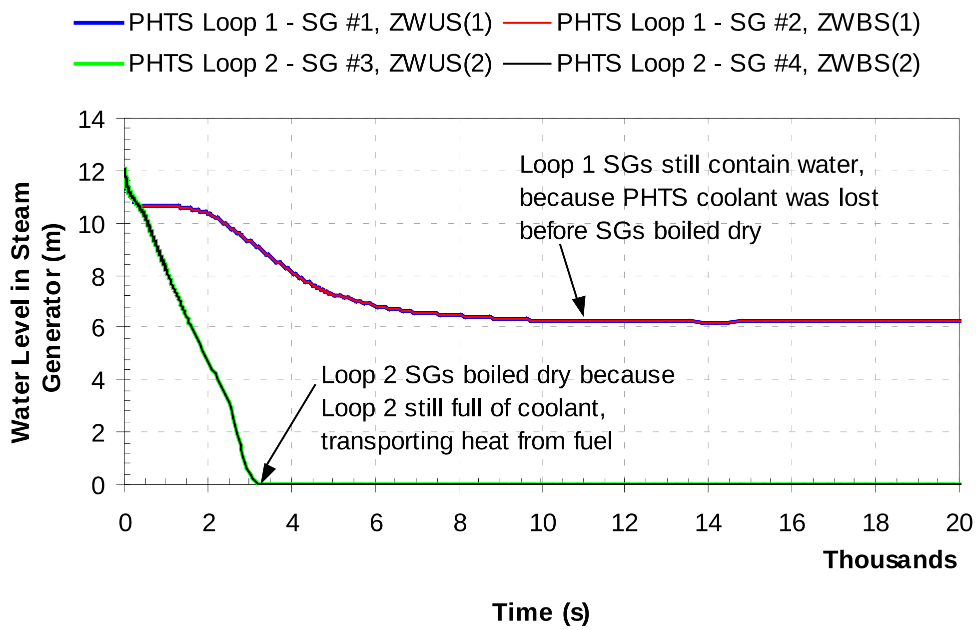

Figure 5 Steam Generator Water Level, Case A (0 – 20,000 s)

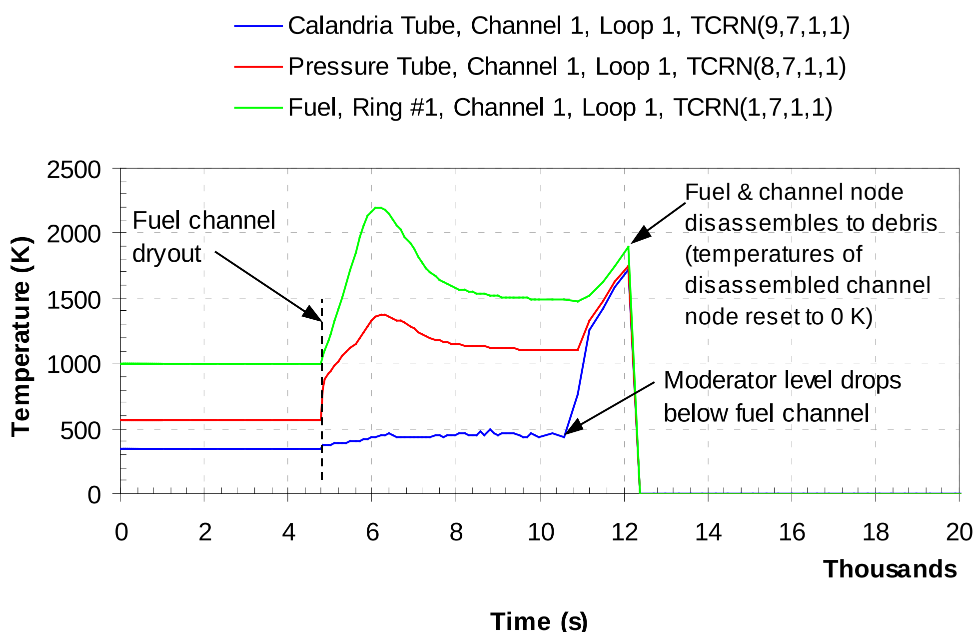

Figure 6 Fuel and Fuel Channel Temperatures, Bundle 7, Channel 1, Loop 1, Case A (0 - 20,000 s)

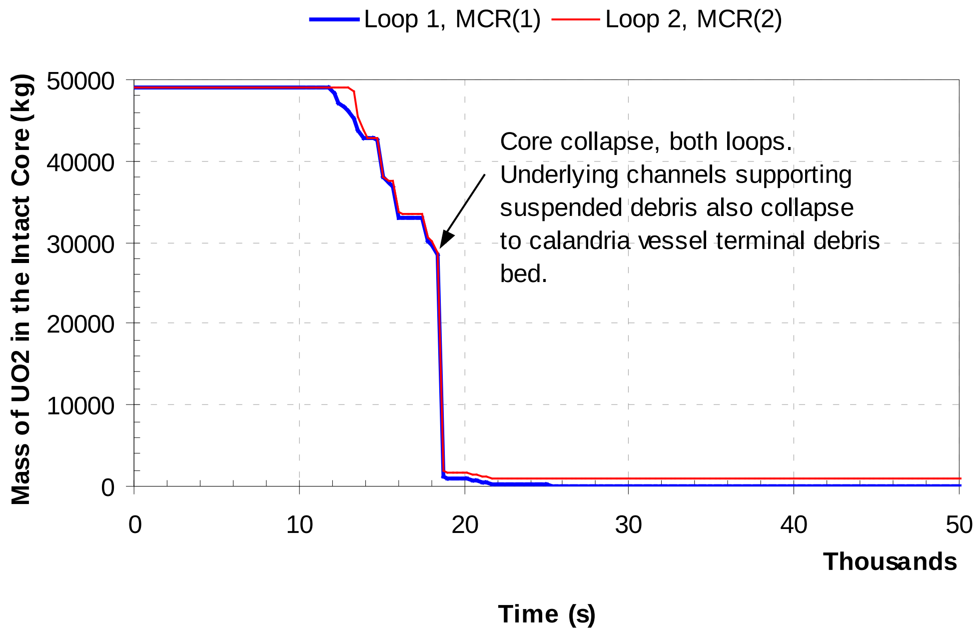

Figure 7 UO_2 Mass remaining in the Intact Fuel Channels, Case A (0 - 50,000 s)

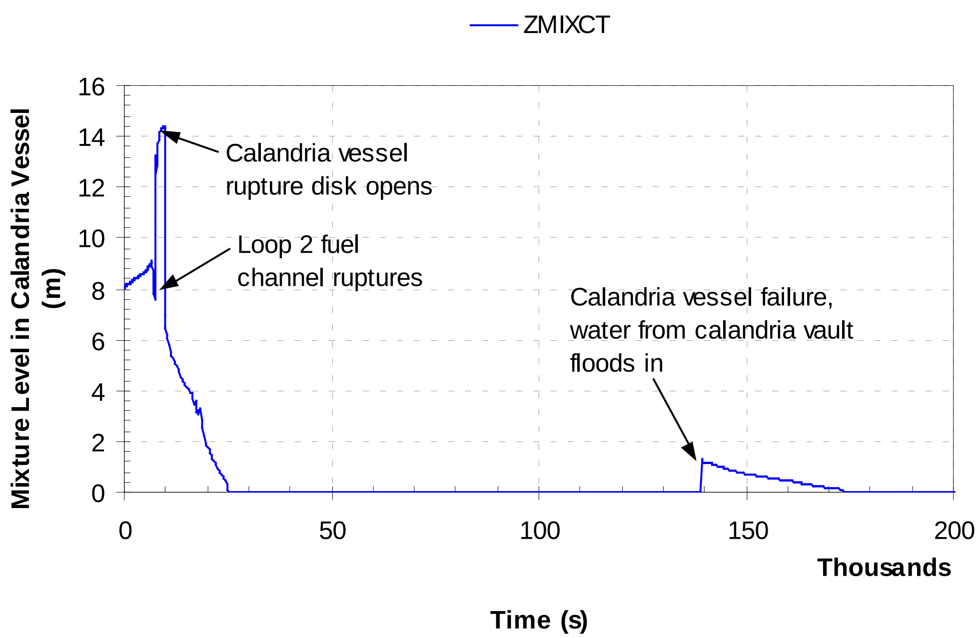

Figure 8 Calandria Vessel Two-Phase Water Level, Case A (0 – 200,000 s)

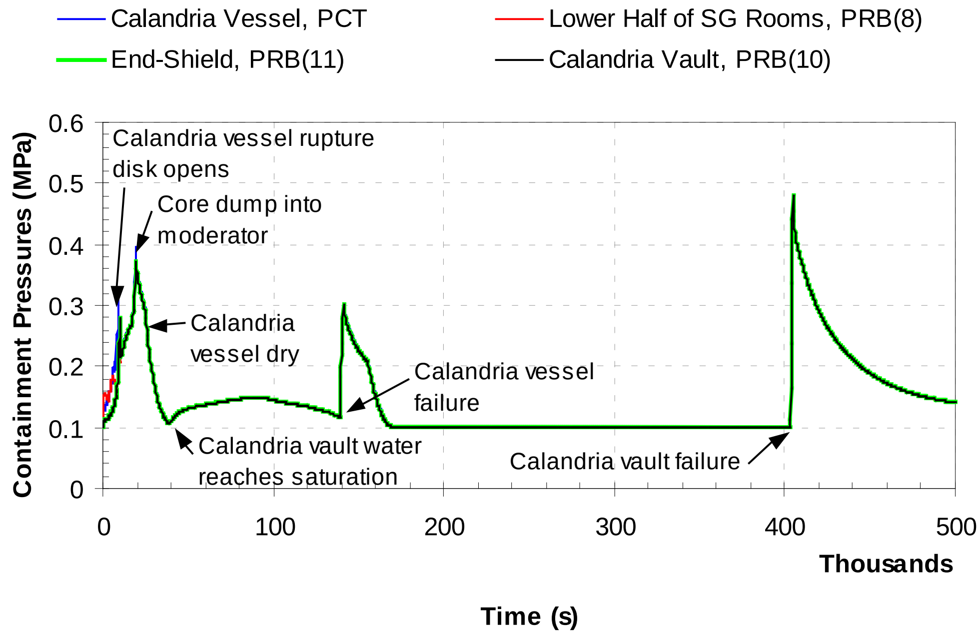

Figure 9 Containment, Calandria Vessel and Calandria Vault Pressures, Case A (0 - 500,000 s)

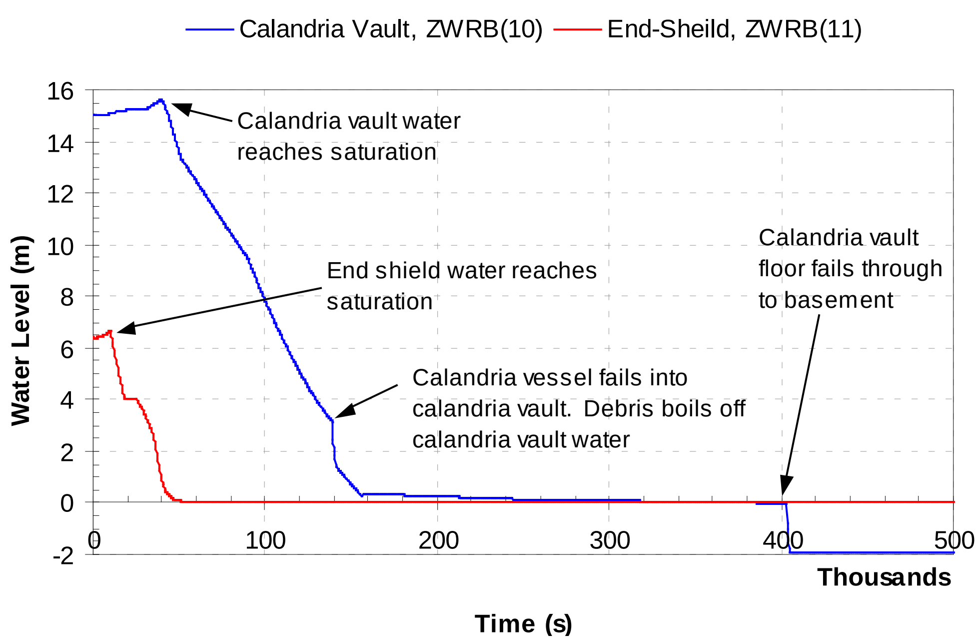

Figure 10 Calandria Vault and End Shield Water Level, Case A (0 – 500,000 s)

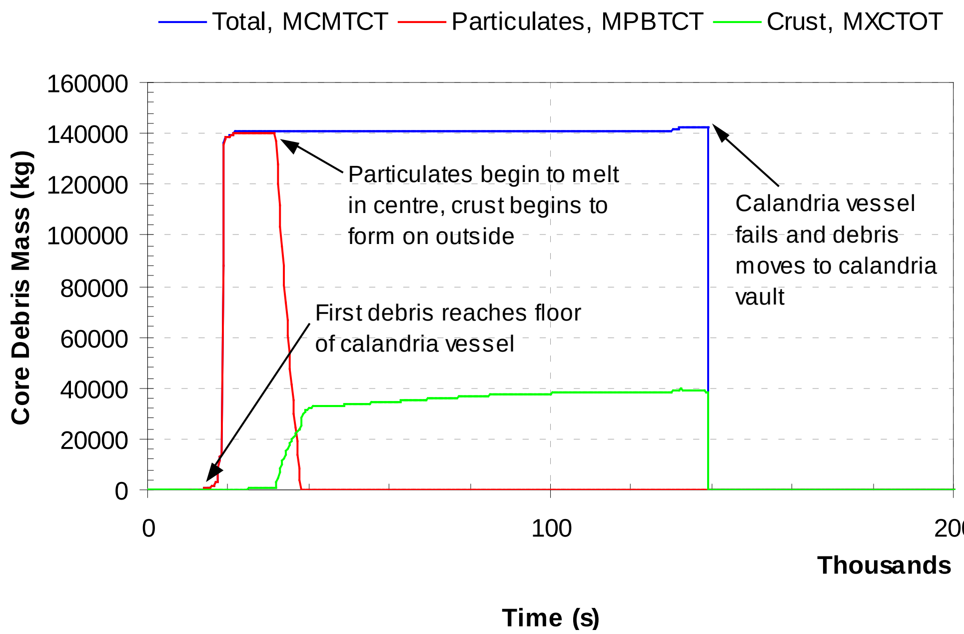

Figure 11 Mass of Corium (Crust, Particulates and Total) in the Calandria Vessel, Case A (0 - 200,000 s)

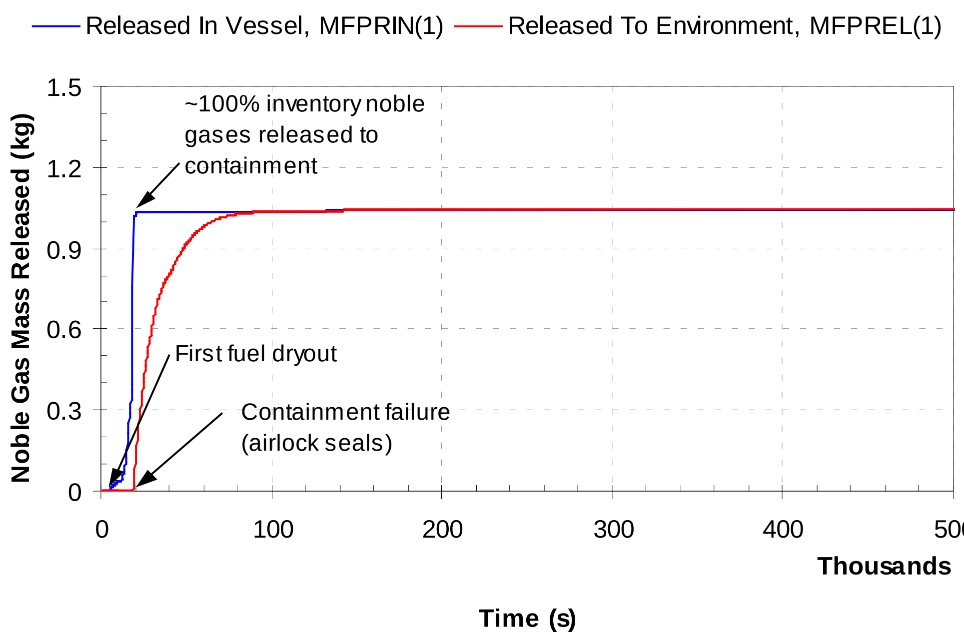

Figure 12 Mass of Noble Gases Released (Active Components Only), Case A (0 - 500,000 s)

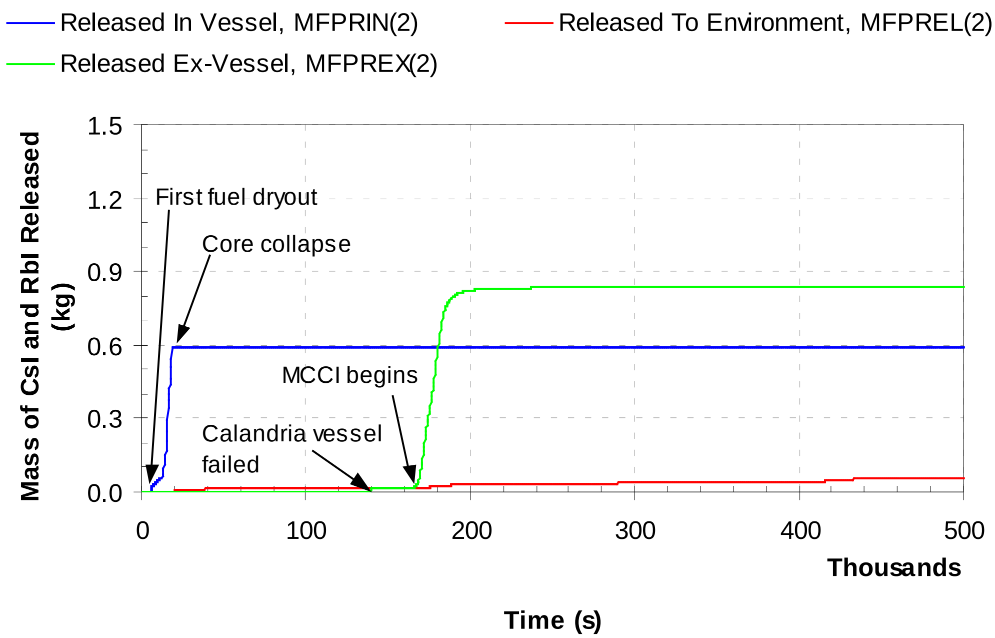

Figure 13 Mass and Location of Iodides Release, Case A (0 - 500,000 s)